A High-Resolution Local Network Study of the Nazca Plate Wadati-Benioff Zone Under Western Argentina

ROBERT F. SMALLEY, JR.[1], AND BRYAN L. ISACKS

*Institute for the Study of the Continents and Department of Geological Sciences,
Cornell University, Ithaca, New York*

This paper presents a precise determination of the fine structure of a Wadati-Benioff zone based on analysis of analog and digital seismic data recorded by a local network in the San Juan Province of western Argentina. The network is located above one of the subhorizontal segments of the subducted Nazca plate. Without the complicating effects of a dipping slab on the locations of earthquakes, the nearly flat geometry of the subducted plate provides an excellent opportunity to determine the thickness and structure of the Wadati-Benioff zone. We found that the depth of the Wadati-Benioff zone beneath the network is 107 ± 5 km. For a set of digitally recorded events, the distance between the shallowest and the deepest event gives a thickness of 20 km, with 90% of the data concentrated in a zone 12 km thick. The spatial distribution of hypocenters shows no evidence of complex internal structure such as a double Wadati-Benioff zone. The local network data also suggest that in the region near 32° S where the dip of the Wadati-Benioff zone changes from flat to steep the Nazca plate flexes rather than tears at depths less than at least 125 km. The intermediate-depth seismicity is separated from an active zone of crustal seismicity by an aseismic region between depths of about 40 and 95 km. The upper surface of the subducted plate, inferred to be at about 90 km, provides an upper limit to the thickness of the South American plate in this region. An apparent westward dip of the Wadati-Benioff zone as determined by the local network data can be accounted for by a 6° westward dip of the Moho beneath the San Juan region, a result that is in agreement with regional gravity and topographic data.

INTRODUCTION

The thickness, morphology, and internal structure of Wadati-Benioff zones places constraints on mechanical and thermal models of subducted lithosphere. Studies based on teleseismic data, while providing good determinations of absolute locations and dips, suffer from the low number of well-located events in any specific area. The use of local network data greatly increases the number of events, but for typical Wadati-Benioff zones, with dips of 30°–50°, the resolution of the structure and thickness of a Wadati-Benioff zone is still degraded by two effects. First, the inclined geometry allows both the depth error and the epicentral error to affect the estimation of thickness of the seismic zone. Second, the three-dimensional velocity structure of the dipping lithospheric slab can have a strong effect on the earthquake locations determined with both local network and teleseismic data. This slab effect is different for the two types of data so that the comparison or combination of these data is complicated [*Barazangi and Isacks*, 1979; *Engdahl et al.*, 1982; *McLaren and Frohlich*, 1985]. An ideal situation would be to obtain data directly above a nearly horizontal Wadati-Benioff zone and thus avoid the effects of a dipping slab.

Two such subhorizontal Wadati-Benioff zones exist beneath western South America, one beneath central Chile/ northwest Argentina and the other beneath central Peru [*Barazangi and Isacks*, 1976], as illustrated in Figure 1. In this paper, we present an analysis of data from a local network operating in the region of San Juan, Argentina, shown

by the box in Figure 1. This network is located directly above a highly active region of the Chile/northwest Argentina subhorizontal zone and thus provides an excellent view of the structure of the Wadati-Benioff zone there. We are able to estimate its depth and thickness, and study its internal structure, from a straightforward analysis of histograms of S-P times of local earthquakes. The epicentral locations are well constrained by the P arrivals recorded across the network, while the time between the P and S arrivals directly determines the hypocentral depth from the essentially vertical ray paths. The velocity anomaly of the subducted slab therefore has little effect on the absolute locations, and epicentral location errors do not project into the thickness estimate. With the direct control on depth given by the local S-P times, the study provides one of the most accurate determinations of Wadati-Benioff zone thickness available.

The map pattern of intermediate-depth seismicity shown in Figure 1 is not uniformly or continuously distributed but is composed of nests and fingers, or bands, of seismicity with large aseismic gaps between the regions of activity. In addition, the dip of the intermediate-depth seismic zone changes markedly several times along strike [*Barazangi and Isacks*, 1976]. Nevertheless, *Bevis and Isacks* [1984] have shown that the seismicity distribution, including the distribution through the region where the dip changes beneath southern Peru, can be fit with a relatively simple surface that is continuous and free of tears. The area of interest in this paper is located in one of the fingerlike patterns of seismicity near 31°S–32°S. This roughly east-west trending linear feature of high seismic activity both defines the flat slab region and forms its southern boundary, separating it from a region of steeper dip to the south that is poorly defined due to the low level of seismicity. The remarkable alignment of this pattern with the inland, or downdip, projection of the aseismic Juan Fernandez Ridge, a

---

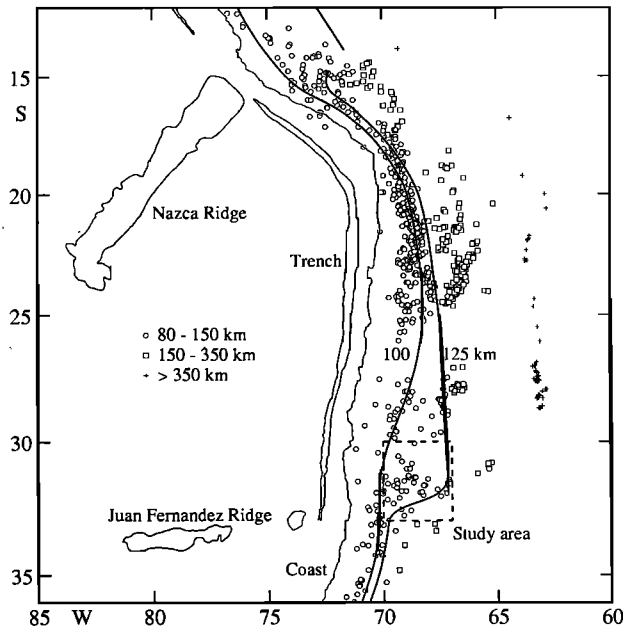[1]Now at Center for Earthquake Research, Memphis State University, Memphis, Tennessee.

Fig. 1. Index map of western South America, with 100- and 125-km depth Wadati-Benioff zone contours (modified from T. Cahill and B. L. Isacks, unpublished data, 1987) and selected ISC epicenters, illustrating the regions of steep and flat subduction. The events selected were located by the ISC using 40 or more stations during the period 1964–1982. South of 32°S there is very little seismic activity at intermediate depths and the selected events between 150- and 350-km depth were located using more than 15 stations. The region of study, marked by the box, is above an active intermediate-depth nest in a finger of seismicity that follows the along-strike projection of the aseismic Juan Fernandez Ridge.

bathymetric feature of the suboceanic Nazca plate, suggests that the seismicity pattern may be related to a continuation of this major structure within the subducted plate. Structures such as aseismic ridges, which are quite common on the oceanic plates, may therefore help cause concentrations of seismicity as they subduct.

The Universidad Nacional de San Juan (UNSJ) has operated a small network in the San Juan region for many years (Figure 2a). Volponi and Marconi [1967] recognized a bimodal character of histograms of S-P times for stations of this network. The bimodal distribution indicates two zones of seismicity. The first zone, with S-P times of 1–4 s, represents shallow seismicity in the crust of the South American plate. The second zone, with S-P times of 11–13 s, is the intermediate-depth Wadati-Benioff zone associated with the subducted Nazca plate. In this paper we analyze data from the seismic network operated by the Instituto Nacional de Prevención Sismica (INPRES) (Figure 2a). The new data from the INPRES network confirm and refine Volponi and Marconi's result and yield a uniquely precise determination of the thickness and structure of the Wadati-Benioff zone.

The INPRES telemetered network in the San Juan region, which began operation in 1977, includes one three-component station (CFA) and six vertical-component stations, with short period (1 Hz) seismometers (Figure 2a). Figure 2b shows locations for 700 well-located intermediate-depth earthquakes, determined using analog data recorded by the INPRES network, for the period January 1984 through September 1985. Figure 2b also shows the selected ISC data

and the 100- and 125-km depth contours of the Wadati-Benioff zone shown in Figure 1. Both contours are based on the selected ISC data, except in the region near 32.25°S, where the change in dip of the seismic zone occurs. There, the 125-km contour is poorly constrained by the few events located by the ISC, and the deformation of the Nazca plate can be interpreted as either a flexure or a tear, represented by continuous or broken contours, respectively [Barazangi and Isacks, 1976; Bevis and Isacks, 1984; Cahill and Isacks, 1985]. A low but significant level of seismic activity is recorded by the local network in this region. The depths of these events suggest that at a depth of 125 km the Wadati-Benioff zone is continuous and the Nazca plate deforms by flexing, as shown by the continuous 125-km contour in Figures 1 and 2b. The region near San Juan is also one of active crustal seismicity. Figure 2c shows 110 well-located crustal earthquakes, located using analog data recorded by the network during the same time period. A cross-sectional view of both the local network data and selected ISC data is shown in Figure 3. The ISC data exhibit the subhorizontal distribution of Wadati-Benioff zone seismicity in the "flat" segment of the subducted Nazca plate between 28° S and 33° S. The cross section also shows the bimodal distribution of seismicity under the network, with no hypocenters between about 40- and 95-km depth.

In the summer of 1984, a digital, event-triggered seismic data acquisition system, designed and built at Cornell, was installed at INPRES. This system records seismic data from the network on magnetic tape at 100 samples/s. The system became fully operational in September 1984 and has run discontinuously since that time, recording about 1/3 the number of events recorded by the analog system. Use of the digital data increases both the accuracy and precision of the measurement of the P and S arrival times. This improvement in the arrival time data results in locations that have smaller rms errors and are more stable. About two dozen events were recorded by both the analog and digital recording systems, and their relative locations are generally less than 5 km apart. In addition to providing better locations, a record section of the digital data convincingly demonstrates a real spread of S-P times, indicative of the thickness of the Wadati-Benioff zone.

WADATI-BENIOFF ZONE STRUCTURE

Method of Estimating Thickness

The S-P time is a direct measure of the distance between a hypocenter and the recording station. Histograms of S-P times recorded at a given station therefore provide data on the distance distribution of events with respect to that station. Volponi and Marconi [1967] constructed histograms of S-P times for the stations of the UNSJ network (see Figure 2a for UNSJ station locations) and found that all the histograms have a large peak between 11 and 13 s S-P time. Figure 4 shows histograms of approximately 1000 S-P times, recorded during the period between January 1984 and September 1985, inclusive, at the INPRES stations RTLL and RTCB (see Figure 2a for INPRES station locations). These histograms also have large peaks near 11 s S-P time and are similar to the histograms of the UNSJ data. The near-constant S-P value of 11–13 s across the UNSJ and INPRES networks, which have apertures of approximately 100 km,
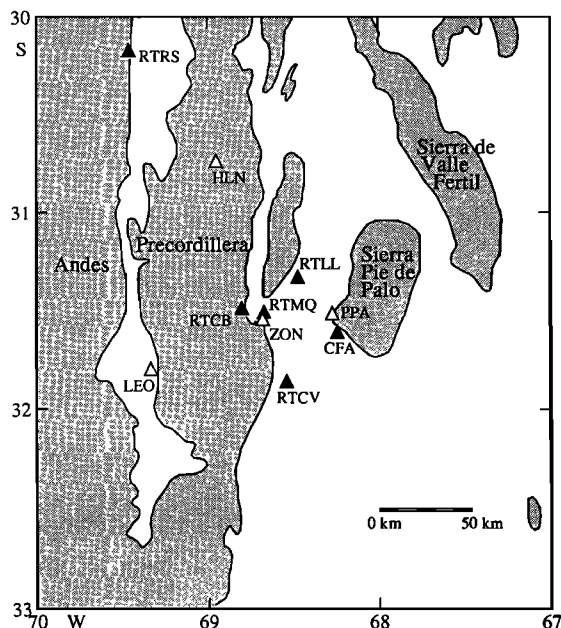
Fig. 2a. Map of INPRES telemetered network (solid triangles) and UNSJ network (open triangles), with station codes. Shaded background represents mountainous areas, and white background sedimentary basins. The Sierra Pie de Palo and Sierra de Valle Fértil are basement block uplifts of the Sierras Pampeanas, while the Precordillera is a thin-skinned thrust belt. The area of this map is outlined by the box in Figure 1.
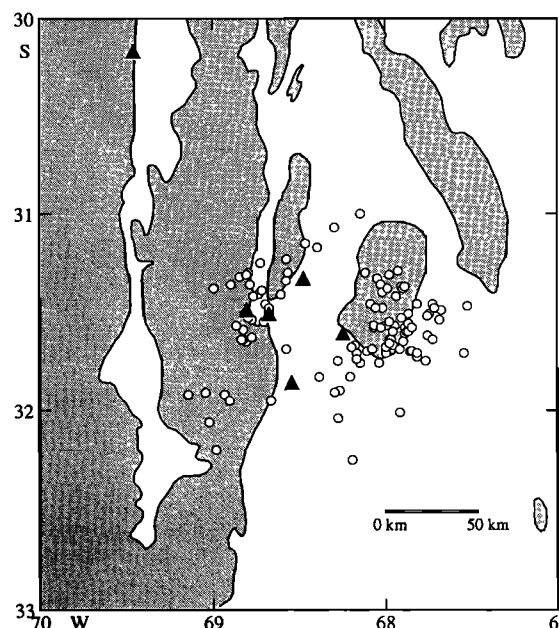

Fig. 2c. Map of 110 shallow epicenters for the period January 1984 to September 1985 located using analog data from the INPRES network. Map and selection criterion are as in Figure 2b. The crustal seismicity is concentrated near the eastern Precordillera, a thin-skinned fold and thrust belt, and Sierra Pie de Palo, one of the Pampean uplifted basement blocks.
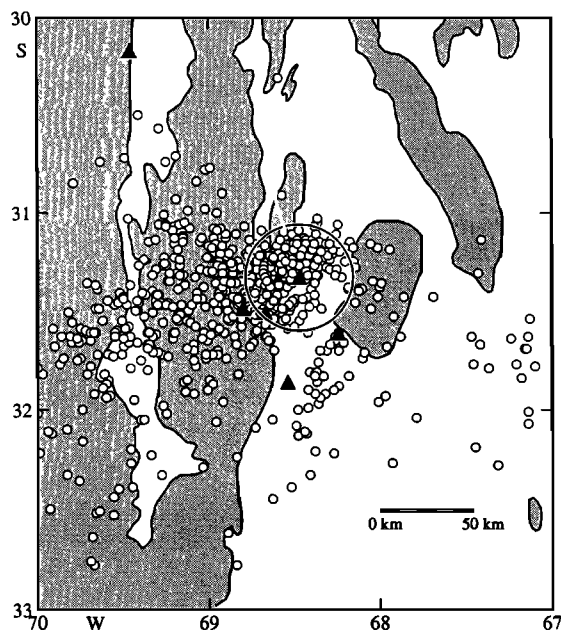

Fig. 2b. Map of 700 intermediate-depth epicenters (open circles) for the period January 1984 to September 1985 located using analog data produced by the INPRES network (solid triangles). The seismicity is concentrated in an approximate east-west zone between 31.1°S and 31.7°S and defines a subhorizontal Wadati-Benioff zone at a depth of about 105 km (Figure 3). The selected events, located using HYPOINVERSE, have four or more P arrivals and two or more S arrivals recorded by the INPRES network, rms errors of less than 0.5 s, and "condition" numbers (ratio of largest to smallest eigenvalue) less than 150. Events within 30 km of the INPRES station RTLL (inside the circle) are used to measure the thickness and structure of the Wadati-Benioff zone based on the S-P times at station RTLL. The selected ISC data (solid circles) and the 100- and 125-km Wadati-Benioff zone contours from Figure 1 are also shown.

implies that the earthquakes have depths of the order of 100 km. Volponi and Marconi were able to locate approximately 40 earthquakes from the UNSJ data. These events display a map pattern similar to that shown in Figure 2b and have a subhorizontal distribution in cross section, with a depth range of 70–100 km.

The structure of the histograms at each station is easily related to the map and cross-sectional patterns of the seismicity. A small peak at S-P times of 1–5 s at stations RTCB (Figure 5), RTMQ, and CFA is produced by nearby crustal earthquakes, at depths of 10–40 km, associated with the Precordillera (near stations RTCB and RTMQ) and the Sierra Pie de Palo (near station CFA), as shown in Figures 2c and 3. These crustal events are also responsible for the gradual buildup of the histograms at stations RTLL (Figure 4) and RTCV between 4 and 8 s. The major peak near 11–12 s at all the INPRES stations is due to the intermediate-depth nest of activity centered under the INPRES station RTLL (Figure 2b). The abundance of 11–12 s S-P times, observed in both Volponi and Marconi's and our study, reflect the high level of seismicity in the intermediate-depth nest, at a depth corresponding to an 11–12 s S-P time. The concentration of activity in this nest also appears stable over a 20-year period.

If an event is located directly beneath a station, the S-P time directly indicates the depth of the hypocenter. For events recorded at epicentral distances that are small compared with their hypocentral depth, the variation of S-P time as a function of epicentral distance is much smaller than the variation as a function of depth. This is demonstrated in Figure 5, which shows the S-P travel time curves for several intermediate source depths, calculated using a model with a single crustal layer over a half space. This figure shows that for hypocentral depths near 100 km, an epicentral offset of
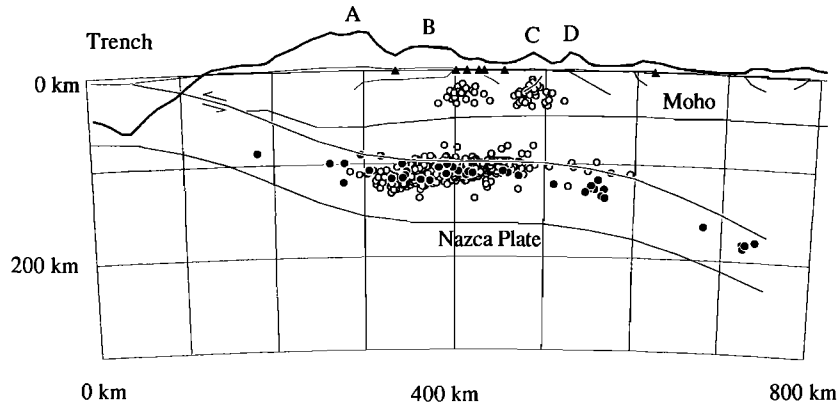
Fig. 3. East-west trending cross section at 31.25°S showing projections of seismicity data, major inferred crustal-scale faults, inferred location of Moho, and swath averaged topography at a scale of 1:1. The topography is also projected at a scale of 10:1. The intermediate-depth hypocenters located with INPRES data and shown in Figure 2b are plotted (open circles) with the selected hypocenters reported by the ISC shown in Figure 1 (solid circles). The widths of the earthquake sections are 160 km for the ISC data and 70 km for the INPRES data. Projections of the INPRES network stations are shown by triangles. The crustal events located by the INPRES network are also projected (open circles). The crustal faults and the inferred position of the Moho are taken from work by B. L. Isacks (manuscript in preparation, 1987), Kadinsky-Cade [1985] and Ortiz and Zambrano [1981]. The east-west topographic profile shows the average elevation of a 100-km-wide swath centered on 31°S. Major topographic features; Main Andes, A; Precordillera, B; Sierra Pie de Palo, C; and Sierra de Valle Fértil, D.

30 km produces a change in S-P time of about 0.5 s. This is roughly the same change in S-P time caused by a 5-km change in hypocentral depth. Thus for a well-located hypocenter with an epicentral distance that is small with respect to its depth, the portion of the S-P time associated with an epicentral uncertainty of 5–10 km is about 0.1–0.2 s, which translates into a precision of about 1–2 km in depth. To study the depth distribution, we therefore examine the distribution of S-P times of a set of intermediate-depth hypocenters that have small epicentral distances from a

given station with respect to their depths. If the spread of S-P times obtained is larger than the "moveout" associated with the epicentral distance range used, then this will either be the result of errors in determining S-P times, or represent a true spread in depths of the events. We can distinguish

Fig. 5. Travel time curves of S-P times for hypocenters with depths between 90 and 125 km and observed S-P times of both the analog and digital data as a function of distance for epicenters within 30 km of station RTLL. The moveout correction discussed in the text is made by "sliding" the S-P times along the appropriate travel-time curve to zero distance, creating a "moveout" corrected S-P time. The moveout corrected S-P times are then used to construct Figure 6. The velocity model used to generate the S-P travel time curves consists of a 40-km-thick crust with a P velocity of 6.4 km/s over a mantle half space with a P velocity of 8.1 km/s, and a measured Poisson's ratio of 1.75. The 188 data for the analog records are shown by open circles, while the 51 data for the digital records are shown by solid circles.

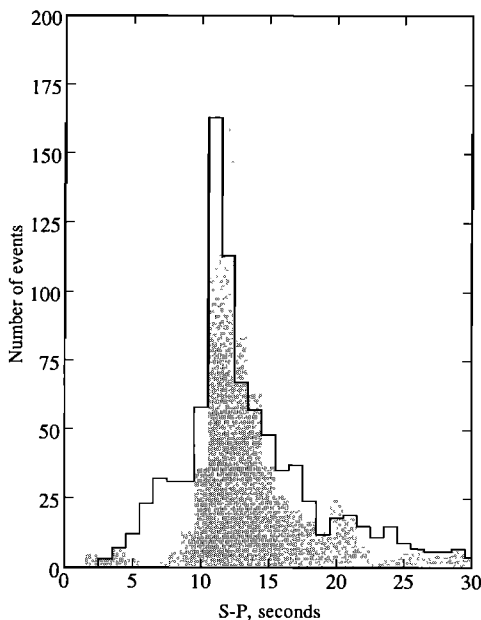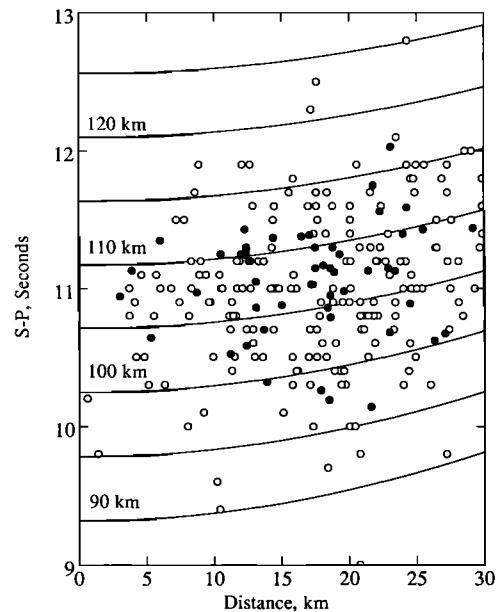Fig. 4. Histograms of all reported S-P times, for the period January 1984 to September 1985, at the INPRES stations RTLL (black line) and RTCB (shaded bars) using a bin size of 1.0 s. During this period, 1377 events had four or more P arrivals and two or more S arrivals at the INPRES network. The number of S-P arrivals for stations RTLL and RTCB shown here are 1036 and 933, respectively.
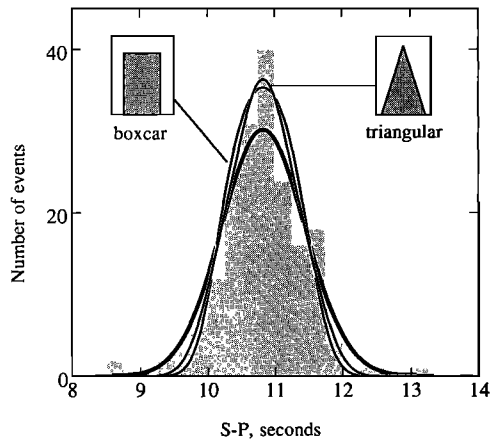
Fig. 6a. Histogram of 188 moveout corrected S-P times, from analog data, of selected intermediate-depth hypocenters with epicentral distances less than 30 km from INPRES station RTLL, using a bin size of 0.25 s. The bin size was chosen based on the magnitude of the uncertainty in determining the S-P time. Also shown are the distributions expected for the three models of S-P distribution discussed in the text. The Gaussian distribution is shown with the heavy line, while the boxcar and triangular distributions, shown schematically in the inserts, are shown by the thin lines. Ninety-five percent of the data are in the region having greater than 3 counts/bin (9.51- to 11.87-s range or 25-km thickness), and 90% are in the region having greater than 4 counts/bin (10.1- to 18.7-s range or 19-km thickness).

between these alternatives by careful examination of the digitally recorded seismograms to assess errors in the determination of S-P times.

Events located below the network can be identified by very high apparent P wave velocities across the network, and locations are then found with HYPOINVERSE [Klein, 1978]. The distribution of S-P times of hypocenters with small epicentral distances from the network is then used to provide a high-resolution view of the vertical structure of the subhorizontal Wadati-Benioff zone. In this geometry the epicenters and depths obtained are weakly dependent on the velocity model used, as discussed above. The range and distribution of the S-P times are therefore direct indicators of the vertical thickness and distribution of seismicity of the Wadati-Benioff zone.

Analysis of Analog Data

Owing to the high level of seismicity in the intermediate-depth nest, it is possible to restrict the region of study to a small area directly below the network station RTLL, where the location precision is very high, and still have enough events to obtain meaningful statistics. In this area the epicentral control is excellent, and the epicenters obtained are relatively insensitive to the velocity models used in locating the events, due to the near-vertical ray paths from the events to the network stations. We will therefore limit the region of study to a circle of 30-km radius (shown in Figure 2b) around the station RTLL. In Figure 5 the S-P times of 188 intermediate-depth events are plotted (open circles) versus epicentral distance. These times were read from analog, vertical-component seismograms from station RTLL. Figure 5 also shows S-P travel time curves for various depths. To construct the histogram of S-P times, we first correct the S-P times for the effect of epicentral distance. The S-P time is corrected for this moveout effect of epicentral distance by

sliding each S-P time along the appropriate travel time curve to zero distance. Figure 6a shows the resultant histogram of moveout corrected S-P times for intermediate-depth events located within 30 km of the station RTLL. The center of the histogram yields the depth, the width gives a measure of the thickness, and the overall shape of the histogram provides information about the distribution of seismicity within the Wadati-Benioff zone. The histogram shows that the S-P times are concentrated near the center, with 95% of the data in a range of 2.4 s, or 26-km thickness, and 90% within a range of 1.8 s, or 19-km thickness. The depth to the center of the zone from the mean value of the S-P times is about 106 km.

Contributions to the width of the histogram include errors in the determination of arrival times, errors in the moveout corrections due to epicentral location errors, and any real variations in depth. The arrival time data reported by INPRES for the analog data are given to 0.1 s. For impulsive P arrivals, the uncertainty is estimated to be ±0.1 s based on examination of seismograms produced by the 1-Hz vertical geophones recorded at 60 mm/min. The contribution of errors in the determination of P arrival time from the analog seismograms to the histogram width is therefore small. The contribution of the uncertainty in epicentral location when making the moveout correction is also a minor effect, less than about 0.1–0.2 s. Determination of the arrival time of the S wave, particularly on vertical-component seismograms, is probably the most significant source of error. While the event-station geometry is excellent for epicenter and depth determination, the near-vertical ray paths are not optimal for obtaining good S arrivals on the vertical-component seismograms. We estimate an uncertainty in the S arrival time of ±0.5 s due to reading error. The magnitude and the source of this error can be examined in more detail using digitally recorded data, as discussed below. The total uncertainty for uncorrelated errors is the square root of the sum of the squares of individual uncertainties and is therefore about ±0.55 s for the analog data.

We are interested in obtaining the contribution to the width of the histogram due to a real spread in the distribu-
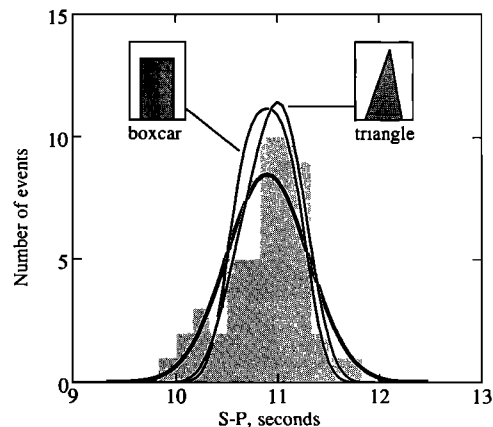

Fig. 6b. Histogram and model distributions for 51 events recorded digitally as in Figure 6a. The bin size is 0.16 s. The inserts show the model distributions schematically. Ninety percent of the data are in the region having greater than 2 counts/bin (10.22- to 11.33-s range or 12-km thickness), and 80% are in the region having greater than 3 counts/bin (10.50- to 11.33-s range or 9-km thickness) .

tion of earthquake depths in the Wadati-Benioff zone, i.e., the real thickness of the zone. We must therefore determine the relative contributions of measurement error and actual zone thickness to the width of the S-P histogram. The moveout corrected S-P times have a mean of 10.83 s and a standard deviation of 0.62 s. A Gaussian with this mean and standard deviation, and an area equal to the area of the measured histogram, is shown in Figure 6a and fits the data rather well. Without additional data on the actual distribution of S-P times, one interpretation of the data is that the seismogenic zone has zero thickness and the width of the histogram is completely due to errors in the determination of S-P times. This interpretation can be argued against by comparing the uncertainty of the S-P time measurement to the uncertainty associated with the Gaussian fit to the S-P data. For a Gaussian error distribution the 95% confidence interval, or uncertainty, is twice the standard deviation and is ±1.24 s for the S-P data. The uncertainty of the S-P time measurement estimated above, however, is ±0.55 s. We therefore conclude that although the measured S-P time distribution can be fit with a Gaussian having a standard deviation of 0.62 s, an interpretation more consistent with the magnitude of the uncertainty of the S-P determination is that the width of the histogram represents a real spread of S-P times. The measured distribution is therefore probably the result of the convolution of a Gaussian error distribution of the S-P time measurement with a nonzero distribution of S-P times.

Given the error distribution, inversion of the measured distribution for the "actual" distribution is a highly ill-conditioned problem and produces nonunique results. It is possible, however, to "fit by eye" some reasonable distributions through forward modeling to obtain some idea of the seismicity distribution. A Gaussian error distribution having a standard deviation of 0.28 s was therefore convolved with several, simple distributions under the constraint that the area of the model distribution be equal to the area of the measured distribution. For a model with a uniform distribution of activity, a boxcar having a width of 1.4 s and centered at 10.83 s produces the "best" fit (Figure 6a) and provides a thickness estimate of 15 ± 3 km. A triangular distribution was also used to model a center weighted distribution. The best fit triangular distribution has a base width of 1.9 s, giving a thickness estimate of 21 ± 3 km. The model thicknesses are in good agreement with the estimates above based on 90% and 95% of the data. The resolution is not high enough, however, to distinguish between the uniform and center weighted distributions.

Analysis of Digital Data

We use the digitally recorded seismograms from the network to study the uncertainties of measuring the S-P times and to show that there is a real spread in the S-P times due to a nonzero thickness of the Wadati-Benioff zone. There are three reasons for the improved resolution available with the digital data. First, the time resolution available on the digital seismograms is 0.01 s, which is much higher than that available on the analog seismograms. Second, using the Lawrence Livermore National Laboratory seismic analysis code (SAC) program, the P arrival time can be picked automatically and systematically, with relative errors of less than ±0.02 s. Third, the S wave phase arrival can be

easily correlated across the network by eye, which improves the S arrival pick. In addition, the station CFA has three components, and the arrival time of S obtained from the vertical component is usually within ±0.05 s of the S arrival as read from the horizontal components. Furthermore, at station CFA, no evidence was found of S to P conversions, which would contaminate the reading of S from vertical component seismograms. We therefore estimate an uncertainty of ±0.2 s for the manual picking of the S arrival time from the digital records. The uncertainty, after including the effect of the moveout correction, is therefore about ±0.3 s.

A histogram of moveout corrected S-P times, for 51 events with epicentral distances less than 30 km from station RTLL and located using the digital data is shown in Figure 6b. This distribution, which has a negative skewness, has a mean of 10.90 s and a standard deviation of 0.40 s. A Gaussian with this mean and standard deviation is also plotted in Figure 6b. As in the case of the analog data, by comparing the ±0.8-s uncertainty of a Gaussian model with the ±0.3-s uncertainty of the S-P determination, we imply a nonzero width for the seismicity distribution. Two model distributions, a boxcar and an asymmetric triangle, were convolved with a Gaussian error distribution having a standard deviation of 0.16 s, and the results are shown in Figure 6b. The fit of the boxcar distribution, which has a width of 0.8 s, or 9 ± 1.5 km, is poor due to the asymmetry of the measured S-P distribution. The asymmetric triangular distribution, which has a base 1.1 s, or 12 ± 1.5 km width, gives an excellent fit to the center of the measured distribution. While the exact shape of the seismicity distribution cannot be obtained, we can conclude that the seismicity distribution is an asymmetric, center weighted distribution.

In the preceding analyses, a nonzero width of the seismic zone was inferred due to the large difference between the uncertainty of the S-P determination and the uncertainty associated with a Gaussian model having a standard deviation equal to the standard deviation of the S-P distribution. Examination of the digital data, however, clearly shows that there is a real distribution in the S-P times and therefore a nonzero width to the seismogenic zone. Figure 7 shows a set of digitally recorded, vertical component seismograms from station RTLL for events with epicentral distances of less than 30 km. The seismograms in Figure 7 are first aligned with respect to the arrival time of P; each seismogram is then shifted left by the moveout correction (determined from the S-P time and epicentral distance), and the seismograms are then arranged in order of increasing S arrival time. If all the events were at the same depth, this moveout correction to the arrival time of P would cause all the S arrivals to fall on a straight, vertical line (note vertical line for reference in Figure 7). The figure, instead, clearly demonstrates the reality of an approximately 1.9-s variation in S-P times. The most important contribution to the width of the S-P histogram is therefore a real spread in the distribution of earthquake depths in the Wadati-Benioff zone, i.e., the real thickness of the zone.

The thickness of the zone, obtained from the 1.9-s range of S-P times (9.9–11.8 s) is 20.5 ± 1.5 km. Two S-P values, however, account for almost 0.5 s of the range, and most of the data (96%) are concentrated in a range of 1.47 s (9.9–11.36 s) for a thickness of 15.8 km. Removing the
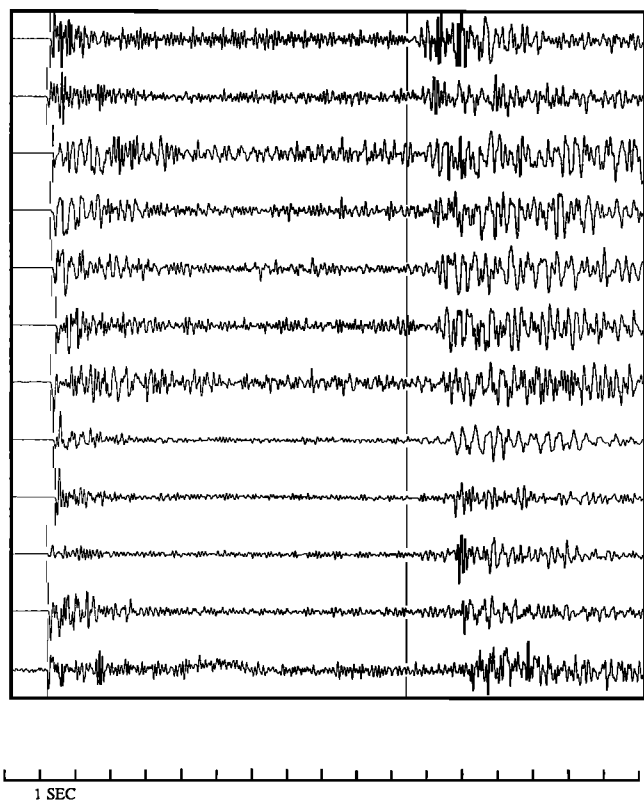
Fig. 7. Selection of digitally recorded, vertical-component seismograms from INPRES station RTLL for some of the earthquakes used to construct the S-P histogram in Figure 6c, arranged by increasing S-P time. Each seismogram is shifted left by the S-P moveout correction for epicentral distance. This figure clearly illustrates that the range of S-P times observed in the histogram of Figure 6c is due to a real depth distribution of the earthquakes and not due to errors in determining the S-P time. The width of the plot is 18 s and the maximum difference of S-P times is 1.9 s. The amplitude of the seismograms has been scaled such that the maximum amplitude of each trace fills the vertical display window.

"tails" of the distribution, which contain one or two counts per bin, leaves 90% of the data in a region 1.1 s or 12 km wide. This estimate is close to the thickness estimate from the asymmetric triangular model. Note, however, that the S-P times in the tails of the distribution are not errors; they appear clearly in the aligned record section of Figure 7 and thus represent a real thickness of the zone. The "center" of the Wadati-Benioff zone obtained from the mean S-P value of 10.9 s from the digital data is 107 km.

Evidence for Moho Inclination

Examination of the cross section in Figure 3 shows an apparent westward dip to the part of the seismogenic zone defined by events located to the west of the local network, which is not seen in the ISC data. This anomalous backwards dip is interpreted as the effect of using a flat layer model in the earthquake location program. The regional topographic profile (Figure 3) implies for simple Airy isostatic models that the Moho under the Precordillera and the main Andean Cordilleras should dip to the west. Gravity data are also in agreement with a westward thickening of the crust [D. Snyder, personal communication, 1985; *Introcaso*, 1980]. Simple ray tracing shows that a 6° westward dip of the Moho, suggested by the topographic and gravity data,

would have the effect of rotating the Wadati-Benioff zone determined by the local network to subhorizontal and brings it into agreement with the dip obtained from ISC data.

DISCUSSION

Thickness of Wadati-Benioff Zones

Estimates of the thickness of various intermediate-depth and deep Wadati-Benioff zones, based on study of the spatial distribution of earthquakes, range from about 10 to 40 km. The studies with the highest resolution have defined three types of Wadati-Benioff zone structures: double-planed zones, zones with faultlike features that are oriented obliquely to the overall geometry of the Wadati-Benioff zone, and thin planar zones with no apparent internal structure.

The clearest example of a double Wadati-Benioff zone is located beneath northern Honshu Island, Japan [*Umino and Hasegawa*, 1975; *Hasegawa et al.*, 1978a, b; *Bevis and Isacks*, 1984]. Each plane has an apparent thickness of 15–20 km, and the centers of the two planes are separated by 30–40 km. Similar double-planed seismic zones have also been reported beneath the Shumagin Islands [*Reyners and Coles*, 1982; *House and Jacob*, 1983] and the Kurile Islands [*Sykes*, 1966; *Veith*, 1974; *Isacks and Barazangi*, 1977] and Tonga [*Kawakatsu*, 1986a]. Several models for these double zones have been proposed, including unbending of the subducted plate [*Isacks and Barazangi*, 1977; *Engdahl and Scholz*, 1977; *Kawakatsu*, 1986b], plate age and convergence rate [*Fujita and Kanamori*, 1981], the stress field generated by the thermal evolution of the plate as it subducts [*House and Jacob*, 1983], sagging of the lithosphere under its own weight [*Sleep*, 1979], and olivine-spinel phase changes [*Veith*, 1974].

Cross-cutting faultlike features within a Wadati-Benioff zone give estimates of seismogenic thickness by resolving the dimensions of these features perpendicular to the inferred overall orientation of the Wadati-Benioff zone. The spatial distribution of multiple events [*Fukao*, 1972; *Wyss*, 1973; *Wyss and Molnar*, 1972] and faultlike features inferred from the spatial distribution of hypocenters and focal mechanism orientations [*Billington and Isacks*, 1975; *Pascal et al.*, 1978] yield estimates of thickness near 35 km, which is close to the total thicknesses of the double Wadati-Benioff zones with both planes taken together. This agreement suggests a seismogenic zone of about 35–40 km within the lithosphere, a zone that probably is related to a cold thermal core in the subducted plate [*Toksöz et al.*, 1971; *Okada*, 1973; *Engdahl et al.*, 1977].

Several intermediate-depth Wadati-Benioff zones defined by high-resolution studies based on local network data, however, are thin single-planed zones. These include southeast Alaska [*Lahr*, 1975; *Pulpan and Frohlich*, 1985], the Adak region of the Aleutians [*Engdahl*, 1973, 1977], New Zealand [*Ansell and Smith*, 1975; *Reyners*, 1980], and southern Peru [*Hasegawa and Sacks*, 1981; *Suárez et al.*, 1983; *Grange et al.*, 1984a, b; *Boyd et al.*, 1984; *Bevis and Isacks*, 1984]. As the experimental resolution increases, the zones at first become narrower until the resolution is sufficient to examine the internal structure of a finite thickness zone. The question then changes from what is the thickness of the intermediate-depth seismogenic zone to

what is its total thickness and what is the internal distribution of seismicity. The total thicknesses for these zones range from 10 to 25 km, with several zones showing a concentration of the activity in the central 5–10 km. Except for a possible center weighted distribution, suggested by the zones that show a concentration near the center of the zone, no clear internal spatial structure, or structure inferred from focal mechanisms, has been resolved in these zones. Our estimated total thickness of 20 km for the seismogenic zone in the subducted Nazca plate is in the range of results reported for other single-planed zones. In addition, our results suggest a center weighted distribution of seismicity, with most of the activity concentrated in the central 12 km of the zone. The age of subducted lithosphere exhibiting thin zones varies from 30–50 m.y. for the Aleutian-Alaskan region to about 100–130 m.y. for New Zealand, a spread that is large and suggests that age is not the factor controlling the differences in thickness reviewed above. It is also interesting that the total thickness estimates for the single-planed intermediate-depth seismic zones, based on high-resolution local network data, are near the estimates of thickness for the individual planes of the double Wadati-Benioff zones.

In this paper we assume that the intermediate-depth seismicity occurs within the subducted Nazca plate. Another model is that the seismicity occurs in an interplate zone of shearing between the two plates. Published focal mechanism orientations [e.g., Isacks and Molnar, 1971; Stauder, 1973; Hasegawa and Sacks, 1981] plus examinations of more recently available solutions of T. Cahill and B. L. Isacks (manuscript in preparation], 1987) argue against an interplate location of the seismicity. Several detailed analyses of the subhorizontal Wadati-Benioff zone beneath southern Peru also provide strong evidence for the location of the seismicity within the subducted plate [Hasegawa and Sacks, 1981; Suárez et al., 1983; Grange et al., 1984a, b; Boyd et al., 1984; Bevis and Isacks, 1984]. A direct measurement of the position of an intermediate-depth event with respect to the slab-asthenosphere contact, using phases reflected from the top of the slab, indicates that the two planes of the double Wadati-Benioff zone in the Kuriles are approximately 15 and 38 km within the subducted slab [Stefani et al., 1982], supporting the model that Wadati-Benioff zone seismicity is intraplate.

Thickness of South American Plate

The Nazca plate at 31°S subducts eastward at a dip of about 30° beneath the western coast of South America to a depth of about 100 km (Figures 1 and 3). The dip then changes to subhorizontal, as the Nazca plate continues to subduct to the east at a dip of approximately 5° for nearly 300 km. The dip then increases to about 30°. In the region of subhorizontal subduction, the position of the subducting Nazca plate places an upper limit on the thickness of the South American lithosphere above it. Assuming that the center of the Wadati-Benioff zone is at 107 km and the zone is 20 km thick, the maximum thickness of the South American plate is 97 km, i.e., the depth to the center of the Wadati-Benioff zone minus one half its thickness. This maximum estimate requires that the Wadati-Benioff zone is at the top of the subducted plate and the bottom of the South American lithosphere is in direct frictional contact with the subducted plate.

Two effects could make the South American lithosphere in this region thinner than this maximum estimate. First, based on thermal modeling and analysis of reflected phases, the Wadati-Benioff zone seismicity is likely to be 5–15 km below the top of the subducting plate in a cool thermal core [e.g., Okada, 1973; Engdahl et al., 1977; Stefani et al., 1982]. Focal mechanisms for intermediate-depth earthquakes in the San Juan region [Stauder, 1973; Triep and de Cardinali, 1984; Dziewonski et al., 1985] show downdip tension, which also indicates that the seismicity is intraplate, i.e., it has some depth in the subducted plate. Location of the seismogenic zone inside the descending plate decreases the estimate of the overriding South American lithospheric thickness by the depth of the seismic zone within the subducted plate. The second factor is the thickness of a presumably hot zone of shearing between the two plates. This zone could include asthenospheric material remaining between the plates from before the development of flat subduction and/or material heated by the effects of a frictional or shear coupling between the plates. The thickness of such a zone is unknown, but an estimate of 5–15 km is not unreasonable. An absolute lower limit of South American lithospheric thickness can be taken as the maximum depth, at about 40 km, of the shallow crustal earthquakes in the San Juan region (Figures 2c and 3).

Assuming the center of the seismogenic zone is 15 km within the Nazca plate and the existence of a 10-km-thick zone of shear heating between the plates, we arrive at an estimate of the thickness of the South American lithosphere of approximately 80 km in the San Juan region. This lithospheric thickness must be incorporated into models of the tectonics of the overlying South American plate, where an active volcanic arc is absent, and the foreland is composed of a topographically low, seismically active region of basement-involved, thick-skinned thrusting that developed east of the Precordillera thin-skinned thrust belt [Allmendinger et al., 1983; Jordan et al., 1983; Jordan and Gardeweg, 1987].

Our 80-km estimate is similar to the lithospheric thickness estimate for the Colorado Plateau based on surface wave, heat flow, and gravity studies [Thompson and Zoback, 1979; Keller et al., 1979]. In contrast to the flat slab region of northwest Argentina, which has an average elevation of less than 1 km, these regions of the western United States are areas of considerable regional uplift. This uplift can be understood as an isostatic response due to the replacement of mantle lithosphere with less dense asthenosphere, i.e., thermal thinning of the lithosphere. In the San Juan region, however, the missing mantle part of the thinned South American lithosphere and the underlying asthenosphere are replaced by the cold, dense lithosphere of the subducted Nazca plate. In terms of isostasy, this could effectively double the thickness of the lithosphere, as suggested by Bird [1984] for the Laramide orogen in early Tertiary time. A thin zone of asthenosphere between the two plates, although serving as a weak zone of concentrated deformation that accommodates the relative horizontal motion of the two plates, also serves to couple the plates in terms of isostatic adjustments [Jischke, 1975; Tovish et al., 1978].

The South American plate in this region is sufficiently weakened compared with a shield or stable platform area that it can be deformed by the ambient lithospheric stresses and the horizontal end load due to convergence with the Nazca plate. The deformation is compressional and is responsible for the large region of crustal seismicity in the Precordillera and the Sierras Pampeanas tectonic provinces [*Allmendinger et al.*, 1983; *Jordan et al.*, 1983; *Kadinsky-Cade*, 1985; R. F. Smalley and B. L. Isacks, manuscript in preparation, 1987].

CONCLUSIONS

Using local network data, we have determined the depth of the center and the thickness of the subhorizontal Wadati-Benioff zone beneath western Argentina to be 107 ± 5 and 20.5 ± 1.5 km, respectively, with most of the seismogenic zone concentrated in a region about 12 km thick. In addition, an internal structure consisting of a simple, triangular distribution of seismicity in the Wadati-Benioff zone is suggested. The Nazca plate is interpreted to be in a state of downdip tension and to be decoupled from the overriding South American plate by a weak zone of asthenospheric or shear-heated material. In the region near 32° S, where the dip of the seismic zone changes from flat to steep, the local network data suggest that to depths of 125 km the Nazca plate is deforming as a flexure rather than a tear. The South American plate is estimated to be 80 km thick, based on the location of the subducted Nazca plate and an inferred decoupling zone between the plates. A 6° westward dip to the Moho under the Andean Cordillera is also inferred, which is in agreement with topographic and gravity data.

REFERENCES

Allmendinger, R. W., V. A. Ramos, T. E. Jordan, M. Palma, and B. L. Isacks, Paleogeography and Andean structural geometry, northwest Argentina, *Tectonics, 2*, 1-16, 1983.

Ansell, J. H., and E. G. C. Smith, Detailed structure of a mantle seismic zone using the homogeneous station method, *Nature, 253*, 518-520, 1975.

Barazangi, M., and B. L. Isacks, Spatial distribution of earthquakes and subduction of the Nazca plate beneath South America, *Geology, 4*, 686-692, 1976.

Barazangi, M., and B. L. Isacks, A comparison of the spatial distribution of mantle earthquakes determined from data produced by local and by teleseismic networks for the Japan and the Aleutian arcs, *Bull. Seismol. Soc. Am., 69*, 1763-1770, 1979.

Bevis, M. G., and B. L. Isacks, Hypocentral trend surface analysis: Probing the geometry of Benioff zones, *J. Geophys. Res., 89*, 6153-6170, 1984.

Billington, S., and B. L. Isacks, Identification of fault planes associated with deep earthquakes, *Geophys. Res. Lett., 2*, 63-66, 1975.

Bird, P., Laramide crustal thickening event in the Rocky Mountain foreland and Great Plains, *Tectonics, 3*, 741-758, 1984.

Boyd, T. M., J. A. Snoke, I. S. Sacks, and A. B. Rodriguez, High-resolution determination of the Benioff zone geometry beneath southern Peru, *Bull. Seismol. Soc. Am., 74*, 559-568, 1984.

Cahill, T., and B. L. Isacks, Shape of the subducted Nazca plate (abstract), *Eos Trans. AGU, 66*, 299, 1985.

Dziewonski, A. M., J. E. Franzen, and T. H. Woodhouse, Centroid-moment tensor solutions for October-December 1984, *Phys. Earth Planet. Inter., 39*, 147-156, 1985.

Engdahl, E. R., Relocation of intermediate depth earthquakes in the central Aleutians by seismic ray tracing, *Nature, 245*, 23-25, 1973.

Engdahl, E. R., Seismicity and plate subduction in the central Aleutians, in *Island Arcs, Deep Sea Trenches, and Back-Arc Basins, Maurice Ewing Ser.*, vol. 1, edited by M. Talwani and W. C. Pitman III, pp. 99-114, AGU, Washington, D. C., 1977.

Engdahl, E. R., and C. H. Scholz, A double Benioff zone beneath the central Aleutians: An unbending of the lithosphere, *Geophys. Res. Lett., 4*, 473-476, 1977.

Engdahl, E. R., N. H. Sleep, and M.-T. Lin, Plate effects in north Pacific subduction zones, *Tectonophysics, 37*, 95-116, 1977.

Engdahl, E. R., J. W. Dewey, and K. Fujita, Earthquake location in island arcs, *Phys. Earth Planet. Inter., 30*, 145-156, 1982.

Fujita, K., and H. Kanamori, Double seismic zones and stresses of intermediate depth earthquakes, *Geophys. J. R. Astron. Soc., 66*, 131-156, 1981.

Fukao, Y., Source process of a large deep-focus earthquake and its tectonic implications-The western Brazil earthquake of 1963, *Phys. Earth Planet. Inter., 5*, 61-67, 1972.

Grange, F. D., P. Cunningham, J. Gagnepain, K. Hatzfeld, P. Molnar, L. Ocola, A. Rodrígues, S. W. Roecker, J. M. Stock, and G. Suárez, The configuration of the seismic zone and the downgoing slab in southern Peru, *Geophys. Res. Lett., 11*, 38-41, 1984a.

Grange, F., D. Hatzfeld, P. Cunningham, P. Molnar, S. W. Roecker, G. Suárez, A. Rodrígues, and L. Ocola, Tectonic implications of the microearthquake seismicity and fault plane solutions in southern Peru, *J. Geophys. Res., 89*, 6139-6152, 1984b.

Hasegawa, A. N., and I. S. Sacks, Subduction of the Nazca plate beneath Peru as determined from seismic observations, *J. Geophys. Res., 86*, 4971-4980, 1981.

Hasegawa, A. N., N. Umino, and A. Takagi, Double-planed structure of the deep seismic zone in the northern Japan arc, *Tectonophysics, 47*, 43-58, 1978a.

Hasegawa, A. N., N. Umino, and A. Takagi, Double-planed deep seismic zone and upper mantle structure in the northeastern Japan arc, *Geophys. J. R. Astron. Soc., 54*, 281-296, 1978b.

House, L. S., and K. H. Jacob, Earthquakes, plate subduction and stress reversals in the eastern Aleutian arc, *J. Geophys. Res., 88*, 9347-9373, 1983.

Introcaso, A., Resultados gravimétricos en la banda latitudinal de Argentina central y países vecinos, *Rev. Geofis., Inst. Panamericano Geogr Hist. Mexico, 12*, 1-25, 1980.

Isacks, B. L., and M. Barazangi, Geometry of Benioff zones: Lateral segmentation and downward bending of the subducted lithosphere, in *Island Arcs, Deep Sea Trenches, and Back-Arc Basins, Maurice Ewing Ser.*, vol. 1, edited by M. Talwani and W. C. Pitman III, pp. 99-114, AGU, Washington, D. C., 1977.

Isacks, B. L., and P. Molnar, Distribution of stresses in the descending lithosphere from a global survey of focal-mechanism solutions of mantle earthquakes, *Rev. Geophys., 9*, 103-174, 1971.

Jischke, M. C., On the dynamics of descending lithospheric plates and slip zones, *J. Geophys. Res., 80*, 4809-4813, 1975.

Jordan, T. E., and M. Gardeweg, Tectonic evolution of the late Cenozoic central Andes, in *Mesozoic and Cenozoic Evolution of the Pacific Margin*, edited by Z. Ben-Avraham, Oxford University Press, New York, in press, 1987.

Jordan, T. E., B. L. Isacks, R. W. Allmendinger, J. A. Brewer, V. A. Ramos, and C. J. Ando, Andean tectonics related to geometry of subducted Nazca Plate, *Geol. Soc. Am. Bull., 94*, 341-361, 1983.

Kadinsky-Cade, K., Seismotectonics of the Chile margin and the 1977 Caucete earthquake of western Argentina, Ph.D. thesis, 253 pp., Cornell Univ., Ithaca, N. Y., 1985.

Kawakatsu, H., Downdip tensional earthquakes beneath the Tonga arc: A double seismic zone?, *J. Geophys. Res., 91*, 6432-6440, 1986a.

Kawakatsu, H., Double seismic zones: Kinematics, *J. Geophys. Res., 91*, 4811-4825, 1986b.

Keller, G. R., L. W. Braille, and P. Morgan, Crustal structure,

geophysical models and contemporary tectonism of the Colorado Plateau, *Tectonophysics, 61*, 137–147, 1979.

Klein, F. W., Hypocenter location program HYPOINVERSE, Part 1, Users guide to versions 1, 2, 3, and 4, *U.S. Geol. Surv. Open File Rep. 78-694*, 1978.

Lahr, J., Detailed seismic investigation of Pacific-North America plate interaction in southern Alaska, Ph.D. thesis, Columbia Univ., New York, 1975.

McLaren, J. P., and C. Frohlich, Model calculations of regional network locations for earthquakes in subduction zones, *Bull. Seismol. Soc. Am., 75*, 397–413, 1985.

Okada, H., Converted *P* phases from the *ScS* phase at the inclined deep seismic zone, *Year Book Carnegie Inst. Washington, 72*, 238–245, 1973.

Ortiz, A., and J. J. Zambrano, La provincia geológica Precordillera oriental, *VIII Congr. Geol. Argent., Actas, 3*, 59–74, 1981.

Pascal, G. B., B. L. Isacks, M. Barazangi, and J. Dubois, Precise relocations of earthquakes and seismotectonics of the New Hebrides island arc, *J. Geophys. Res., 83*, 4957–4973, 1978.

Pulpan, H., and C. Frohlich, Geometry of the subducted plate near Kodiak Island and Lower Cook Inlet, Alaska, determined from relocated earthquake hypocenters, *Bull. Seismol. Soc. Am., 75*, 791–811, 1985.

Reyners, M., A microearthquake study of the plate boundary, North Island, New Zealand, *Geophys. J. R. Astron. Soc., 63*, 1–22, 1980.

Reyners, M., and K. S. Coles, Fine structure of the dipping seismic zone and subduction mechanics in the Shumagin Islands, Alaska, *J. Geophys. Res., 87*, 356–366, 1982.

Sleep, N. H., The double seismic zone in downgoing slabs and the viscosity of the mesosphere, *J. Geophys. Res., 84*, 4565–4571, 1979.

Stauder, W., Mechanism and spatial distribution of Chilean earthquakes with relation to subduction of the oceanic plate, *J. Geophys. Res., 78*, 5033–5061, 1973.

Stefani, J. P., R. J. Geller, and G. C. Kroeger, A direct measurement of the distance between a hypocenter in a Benioff-Wadati zone and the slab-asthenosphere contact, *J. Geophys. Res., 87*, 323–328, 1982.

Suárez G., P. Molnar, and B. C. Burchfiel, Seismicity, fault plane solutions, depth of faulting and active tectonics of the Andes of Peru, Ecuador, and southern Columbia, *J. Geophys. Res., 88*, 10,403–10,428, 1983.

Sykes, L. R., The seismicity and deep structure of island arcs, *J. Geophys. Res., 71*, 2981, 1966.

Thompson, G. A., and M. L. Zoback, Regional geophysics of the Colorado Plateau, *Tectonophysics, 61*, 149–181, 1979.

Toksöz, M., J. Minear, and B. R. Julian, Temperature field and geophysical effects of a downgoing slab, *J. Geophys. Res., 76*, 1113–1138, 1971.

Tovish, A., G. Schubert, and B. P. Luyendyk, Mantle flow pressure and the angle of subduction: Non-Newtonian corner flows, *J. Geophys. Res., 83*, 5892–5898, 1978.

Triep, E. G., and C. B. de Cardinali, Mechanismos de sismos en las Sierras Pampeanas occidentales, Actas III, 61–80, Nov. Congr. Geol. Argent., S.C. de Bariloche, 1984.

Umino, N., and A. Hasegawa, On the two-layered structure of deep seismic plane in northeastern Japan arc (in Japanese), *Zizin, 28*, 125–139, 1975.

Veith, K. F., The relationship of island arc seismicity to plate tectonics, Ph.D. thesis, Southern Methodist Univ., Dallas, Tex., 1974.

Volponi, F., and H. Marconi, On the spatial distribution of earthquakes near San Juan, Argentina, *Year Book Carnegie Inst. Washington, 66*, 37–42, 1967.

Wyss, M., The thickness of deep seismic zones, *Nature, 242*, 255–256, 1973.

Wyss, M., and P. Molnar, Source parameters of intermediate and deep focus earthquakes in the Tonga arc, *Phys. Earth Planet. Inter., 6*, 279–292, 1972.

B. L. Isacks and R. F. Smalley, Jr., Institute for the Study of the Continents and Department of Geological Sciences, Cornell University, Ithaca, NY 14853.